

BME SENIOR CAPSTONE PROJECT

Understanding the Impact of cECM Peptides on Cardiac Wound Healing and Identifying their Mechanism

Bailey Levin, Ryan Rockett, and Joseph Pizzi

In collaboration with Lauren Black

Abstract:

It has been shown that the fetal/neonatal cardiac extracellular matrix (cECM) can promote neonatal rat cardiomyocyte proliferation in vitro more effectively than neonatal or adult ECM. Understanding the interactions that inhibit proliferation as organisms age could be used to induce proliferation post-injury. The peptide fibrillin-1-region-1(F1R1), a specific region of matrix component fibrillin-1, has been shown to improve the wound-healing capabilities of iPSC-derived cardiomyocytes. However, the underlying biological mechanism behind the effects of F1R1 and these other fibrillin-derived peptides is a black box. It was also observed that it has sequential homology with a latent binding protein of TGF- β , a growth factor that inhibits hematopoiesis and induces cardiac fibroblasts to produce scar tissue. So, the first steps are to observe the interactions between F1R1 and TGF- β in neonatal cardiac fibroblasts to see if inhibiting TGF- β -induced scar tissue formation is how F1R1 achieved cardiomyocyte proliferation. After this, the downstream targets affected by F1R1 treatment in cardiac fibroblasts will be determined. In this, the lysate of cells treated with F1R1 will be compared to that of untreated cells using a Western Blot, with antibodies labeling proteins in the activation pathway typically engaged by TGF- β . Overall, the project seeks to characterize how fibrillin-1 liberated peptides can elicit neonatal regeneration and determine if these mechanisms can be translated to mature tissue to lay the groundwork for an in vivo, protein-based therapeutic for cardiac injury and congenital heart defects.

Keywords:

Cardiac Fibroblast, Regeneration, Extracellular Matrix

ENGINEERING DESIGN ELEMENTS:

The central aspect of this project that was designed is the experimental setup and subsequent analysis. In this, the experimental treatment groups and staining methods were chosen such that meaningful data on the biological pathway of cardiac cell proliferation and differentiation could be gleaned. In the later stages of the project, the focus shifted to designing experiments that identify which signaling proteins are affected by F1R1 treatment to suppress the fibrotic phenotype in cardiac fibroblasts. Here, the design of an antibody panel with proteins relevant to TGFb-induced fibroblast activation was our top priority. We also chose statistical analysis techniques like post hoc testing to help contribute toward the understanding of the role of these cECM peptides in cardiac cell proliferation or reveal patterns that lead to further experimentation.

Our first objective was to determine if/how F1R1 interacts with TGF-B to promote neonatal cardiomyocyte regeneration. Through sequence homology analysis, it was found that F1R1 was structurally similar to latent TGF-B binding protein 2 (LTBP2)¹. TGF-B negatively regulates proliferation, as it induces cardiac fibroblasts to differentiate into myofibroblasts, whose primary function is to engage in fibrosis and scar tissue generation. In the context of injury response, this interaction between TGF-B and cardiac fibroblasts is not ideal, as it fills the void left by cardiac cell death events with non-contractile tissue. So, it is hypothesized that in the neonatal cell environment, F1R1 may bind to TGF-B, preventing it from activating cardiac fibroblasts and therefore promoting proliferation by inhibiting fibrosis. The second major objective was to figure out what TGF-b signaling proteins in cardiac fibroblasts are influenced by F1R1 treatment. A Western blot comparing the abundance of proteins, indicated by band intensity, involved in fibroblast activation (SMAD family, Akt/PI3k, MAPK family, mechanoreceptor-associated proteins, etc.) between F1R1 treated cells and the control would help reveal how F1R1 counteracts the fibroblast-myofibroblast transition^{2, 3, 4, 5}. The final objective was to determine the influence of F1R1 when it is increased to a concentration beyond physiological standards. It has been shown that the natural concentration of F1R1 is 50 ug/ml in cardiac tissue.

In order to explore the phenotypical relationship of F1R1 and TGF-B, it was necessary to use methods that can properly demonstrate their function. Cell cultures of cardiomyocytes and cardiac fibroblasts were produced by isolating cardiac cells from rat pups. For these cultures, cell viability assays were performed using trypan blue staining to confirm that an adequate level of growth had been achieved. This assay also provides the concentration of cells in media, which was then used to calculate the volume of cell solution required per plate. CellProfiler software was used in tandem with Ki67 and alpha-smooth muscle actin (aSMA) staining to calculate the number of proliferating and differentiating cells in the culture. To execute the second aim, a Western blot of F1R1-treated fibroblast lysates would be performed to qualitatively show the difference in labeled protein abundance. Before this, a BCA assay was done to quantitatively measure the total protein content in the lysate of each experimental condition to allow for comparison. Further data analysis will be recorded and analyzed using MATLAB and Excel.

To test the relationship between F1R1 and TGF-B, experimental groups with F1R1 were tested against positive and negative constants. The extent of cardiac fibroblast proliferation was represented using Ki67 staining while the extent of the culture's differentiation was evaluated using aSMA staining. With CellProfiler, the extent of proliferation and differentiation was characterized quantitatively alongside cell number. Regarding our main hypothesis, the TGF-B group had high aSMA stain intensity in the first experiment, and the group with both TGF-B and F1R1 showed comparably reduced aSMA staining closer to the control. Specifically, a highlighted comparison was between aSMA levels in the TGF-B-only group and the combined group. This revealed the degree to which F1R1 inhibits the differentiation of fibroblasts into myofibroblasts through TGF-B binding when compared to TGF-B stimulation alone. For the western blot experiment, the main quantitative deliverable was planned to be the fold change in certain activation-associated signaling proteins. The expected difference would vary depending on the protein, but we would expect to see a 2-fold decrease in SMAD family protein abundance and a 1.25-fold

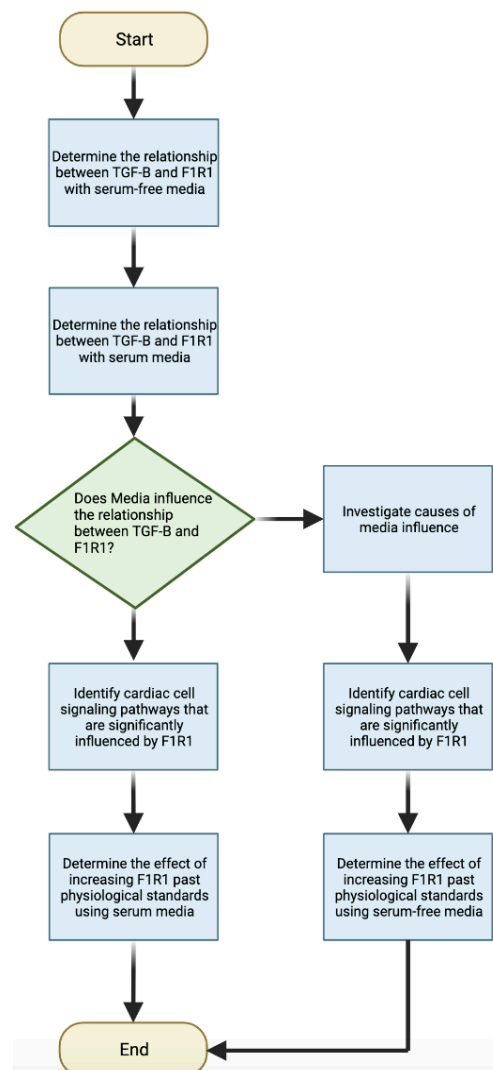
decrease in pAKT/AKT based on previous experiments with TGF- β and cardiac fibroblasts⁶. In regards to the F1R1 dose dependency experiment, the primary objective was to see if supraphysiological concentrations of F1R1 would produce an even more potent anti-fibrotic effect. With this, the standard 50 μ g/mL concentration would be tested against both 100 μ g/mL and 200 μ g/mL concentrations of F1R1 in TGF β -stimulated cells and the resulting aSMA staining would act as an indicator of differentiation.

Rodents play a key role in cardiovascular research due to their convenience, cost, and detectability of physiological indicators⁷. Through extensive testing, rodent models have become a well-defined research tool. Because of the listed advantages and established testing protocols, we used rat models for in vitro testing. The drawbacks of using a rodent model include differences in gene expression profiles and unsynchronized embryo development⁷. We do not think these variations had a large impact on our results. Rodent models are often used in literature to represent the impact of Fibrillin-1 with small differences in the function of Fibrillin-1 in the organism compared to humans⁸. The timing of embryo development should not impact our research as the neonatal and fetal rats showed similar results in previous proliferation studies. However, future studies will be needed with human tests to confirm the findings of our research before use in therapeutics.

The utilized methods also involved working with live cell cultures. This required a base cost to produce these cultures as well as constant input to maintain them over a period of testing. Costs also arose from the devices used to analyze the culture data like the Keyence and its changing availability. Since the study was performed in an environment with live tissue, biosafety was an important factor to consider. Other key constraints we had to take into account were the time investment and scope. As we learned, the depth of the project had to be achievable within two semesters, and since experimentation deals with cell cultures, clearly defining and abiding by timelines was very important. Project deliverables were constantly reevaluated based on our changing expectations with each experimental iteration and the setbacks that came with them.

An alternative approach that was considered was eliciting *in vivo* cardiomyocyte regeneration by targeting the gene expression of cardiac fibroblasts. These cells manufacture the cECM, changing its composition as tissue matures and eventually losing its ability to regenerate. With gene editing, the genes in cardiac fibroblasts that mediate their shift in function from creating a proliferation-promoting matrix composition to prioritizing fibrosis could be targeted. However, gene editing platforms like CRISPR can be expensive and have off-target mutational effects, so the current path of using matrix-derived peptides themselves as a therapeutic has been pursued instead for now.

Upon reflecting on the goals set at the start of each semester, the planned scope of our project was overly ambitious. At the end of the fall semester, the relationship between F1R1 and TGF β in influencing cardiac fibroblast activation was established through initial experimentation in serum-free media. With this success, we anticipated being able to do a western blot to learn about the cellular targets of F1R1, after which we could move on to the impact and mechanism of F1R2 (fibrillin-1



region 2). However, upon discussion with senior lab members, the high basal differentiation in the control of our first experiment could not be ignored. Due to this advice, we quickly pivoted to re-doing last semester's F1R1/TGFb experiment but with fibroblasts cultured in serum-containing media instead to curb control differentiation. Here we encountered some difficulties, with the first run of this experiment failing to produce an adequate amount of cells to analyze due to procedural errors. As a result, the planning and execution of the F1R1 western blot experiment were delayed to much later in the spring semester. By the time an antibody panel was composed, finalized, and then purchased, the end of the semester was rapidly approaching. After collecting lysate from F1R1-treated, scrambled F1R1-treated, and untreated cells, it took some time to obtain access to the plate reader for the BCA. Unfortunately, even after the BCA was performed, the lysate protein samples were too dilute to perform the blot adequately. When quickly pivoting to an F1R1 dose-dependency experiment to try and get more data, our culture became unintentionally poly layered and the images taken could not be used for analysis. While we did not get far in determining the mechanism of F1R1, its antagonistic relationship with TGFb-induced fibroblast differentiation was well established and further experiments have been planned.

Engineering Design Table

	General Objective	How aims will be achieved	Key Deliverables	Validation
Short-Term (F1R1)	Determine the proliferative mechanism of F1R1 in the neonatal setting - is promotion induced by inhibitory action on TGF-B?	Experimental treatment of neonatal cardiac fibroblasts w/ TGF-B + F1R1. Expecting Decreased differentiation into myofibroblasts in TGF-B + F1R1 group when compared to TGF-B alone (less scar tissue)	% of cells staining for aSMA and Ki67 - indicates myofibroblast activity	TGF-B + F1R1 % aSMA should be less than TGF-B % aSMA Control: 24% TGF-B: 80% TGF-B + F1R1: 24% ¹⁶ and TGF-B + F1R1 % Ki67 should be greater than TGF-B % Ki67 Control: 14.8% TGF-B: 9.5% TGF-B + F1R1: 14.8% ¹
Mid-term (What's next)	Understand what pathways F1R1 targets in cardiac fibroblasts to counteract activation signaling.	Western blot and BCA assay of F1R1 treated and untreated fibroblasts in both the presence and absence of TGF-b. The chosen antibodies will be associated with the myofibroblast transition. The full antibody panel is as follows: <ul style="list-style-type: none">- SMAD 2/3- pSMAD 2/3- Akt- pAkt- YAP- TAZ- RhoA- pROCK1- p38 MAPK- ERK 1/2	Fold change in selected proteins associated w/ differentiation between the F1R1-treated and control groups. This will be determined by performing a quantitative analysis of Western blot antibody staining intensity. A BCA assay will be used alongside this to compare total protein concentration across experimental groups.	Smad, Akt, MAPK, PI3k, and other differentiation-linked signaling proteins should have a decreased abundance in the F1R1-treated cells. The extent of this will depend on the protein in question. pAKT/AKT: 2-fold decrease in quantity from TGFb to TGFb/F1R1 ⁶ . SMADs (broadly): 1.25-fold decrease in quantity from TGFb to TGFb/F1R1. YAP/TAZ :~2-fold increase in quantity from TGFb to TGFb/F1R1 ²⁴ . RhoA/ROCK1: 2-fold decrease from TGFb treated to F1R1/TGFb treated ²⁵ . p38 MAPK: 2-fold decrease from TGFb to TGFb/F1R1 treated ²³ .

		- GADPH (control)		ERK 1/2: ~2-fold decrease from TGFb to TGFb/F1R1 ⁴
Long-term (beyond this semester)	Characterize transcriptome changes induced by F1R1 in cardiac fibroblasts that lead to an anti-fibrotic phenotype.	RNA-seq of F1R1-treated and untreated cardiac fibroblasts.	Fold change in gene expression from the control to F1R1 experimental groups. The only anticipated result is that genes corresponding to the fibroblast to myofibroblast transition should be expressed less after the F1R1 introduction.	Genes key to the differentiation process should be downregulated in the F1R1 group when compared to the control. RASL11B: 5-fold decrease from control to F1R1 ²⁶ . XYLT1: 6-fold decrease from control to F1R1. COMP: 5-fold decrease from control to F1R1

INTRODUCTION

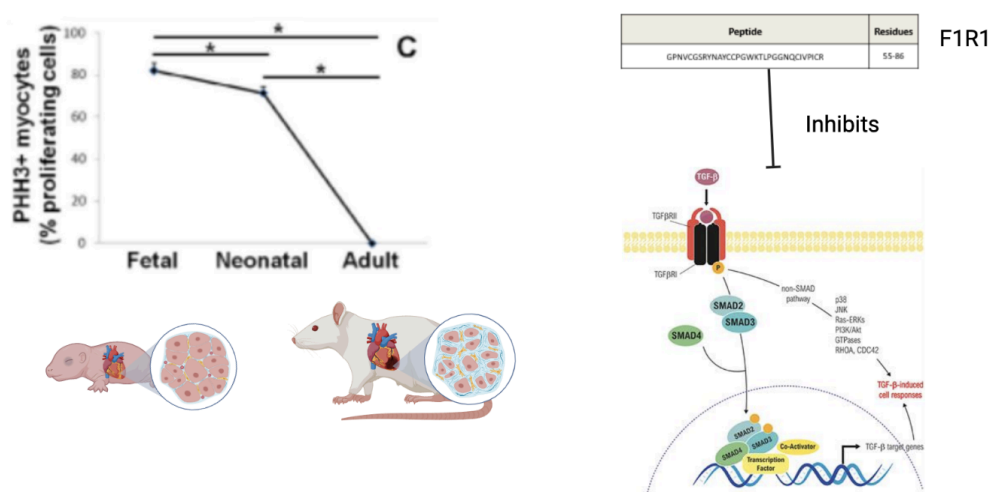
With the rising prevalence of cardiovascular disease, the need for regenerative treatments that facilitate cardiac wound healing has become more pronounced. Specifically, congenital heart defects (CHD) are a type of cardiovascular disease that exhibit a wide range of structural abnormalities, including defective valves and malformed atria/ventricles, that can lead to a lack of adequate blood circulation throughout the body⁹. Another potential consequence of heart conditions is heart failure, which still has high mortality among patients despite recent advances in regenerative therapies¹⁰. In both cases, the root issue lies in the lack of regenerative properties exhibited in mature heart tissue after cardiomyocyte loss. Without a way to self-renew, dead cardiomyocytes are effectively replaced with cardiac fibroblasts that engage in fibrosis, which does nothing to recover the loss of contractile tissue¹⁰. In the context of heart donor scarcity, there is a high demand for an *in vivo* therapeutic that can effectively elicit cardiomyocyte regeneration. Unfortunately, current methods for a treatment like this have fallen short. Approaches like reprogramming cardiac fibroblasts into cardiomyocytes or promoting proliferation genes with microRNA have shown promise, but full tissue integration and controlled proliferation have yet to be achieved^{11,12}. One path to developing a treatment like this lies in the rate of wound healing seen in fetal and neonatal heart tissue. It has been shown in numerous mammals that differentiating heart tissue has incredible regenerative potential, allowing for injured or diseased hearts to recover their function¹³. However, as cardiomyocytes mature, they exit the cell cycle, and cell death events cause long-lasting tissue damage. So, a major objective in the field of cardiac regeneration is to figure out why developing heart cells have this proliferative potential and how relevant biological mechanisms could be targeted to elicit a similar response in matured tissue.

In the Black lab, this subject is being explored by better defining the relationship between cardiac ECM (cECM) peptides and a more proliferative post-injury response. Through liquid chromatography-mass spectroscopy (LC-MS), initial studies identified that certain ECM elements, like fibrillin I, were more abundant in fetal and neonatal hearts¹⁴. Additionally, PHH3 staining indicated that significantly more cardiomyocytes were dividing on fetal cECM when compared to the other conditions. These findings suggested that the matrix composition of fetal and neonatal hearts facilitates increased cardiomyocyte proliferation. In subsequent experiments, fetal and adult cECM peptides were separated by molecular weight using gel electrophoresis, after which neonatal cardiac cells were cultured directly on the gel¹. In this, immunostaining showed regions/peptides on the gel that induced significant proliferation in the cultured cells. These peptides of interest were then analyzed using LC-MS, revealing that molecular weight regions with heightened proliferation had a greater amount of peptides derived from matrix

component fibrillin-1. In fact, all four fibrillin-1 sequences associated with cardiomyocyte proliferation were clustered near the N-terminus of the protein.

To follow up on these previous findings, we are now focused on studying the mechanisms underlying the proliferative increase brought on by the four identified fibrillin-1-derived peptides. For the first peptide region (F1R1), computational analysis has revealed that it demonstrates high sequence homology with Latent TGF- β binding protein 2 (LTBP2)⁶. TGF- β has been linked to the differentiation of cardiac fibroblasts into myofibroblasts, which then engage in fibrosis and facilitate scar tissue formation post-injury¹⁵. This suggests that F1R1 may promote cardiomyocyte proliferation in neonatal tissue by inhibiting TGF- β and therefore myofibroblast scar tissue generation. After verifying the effects of F1R1 on TGF- β stimulation, the specific protein targets of F1R1 that lead to hampered fibroblast activation can be explored. In this, a Western blot experiment comparing the presence of different proteins involved in the myofibroblast transition between F1R1-treated cells and an untreated group could reveal what proteins F1R1 acts on or influences. Specifically, the Smad 2/3/4 complex formed after TGF- β binding regulates gene expression to promote fibroblast differentiation into myofibroblasts². Fibroblast activation can be alternatively initiated by SMAD-independent signaling, where proteins like ERK 1/2, PI3K/Akt, and MAPK p38 participate in differentiation signal propagation^{16, 4}. Aside from TGF- β stimulation, differentiation can also be influenced by fibroblast mechanosensing, where the activities of proteins like RhoA/ROCK1 and YAP/TAZ are altered to induce differentiation in the presence of mechanical stress^{4, 5}. Consequently, antibodies for SMADs, MAPKs, and proteins downstream of mechanoreceptors will be used in the Western blot to see how F1R1 affects TGF- β -mediated activation and increased matrix production. Any other cellular mechanisms affected by F1R1 will be shown in a subsequent RNA-seq experiment, which will characterize how the cardiac fibroblast transcriptome changes when F1R1 is introduced. By understanding how developmental cECM peptides facilitate cardiomyocyte proliferation post-injury, relevant pathways could be targeted in mature tissue to overcome the regulatory mechanisms preventing cardiomyocyte cell cycle re-entry. This could lay the groundwork for an *in vivo* protein-based therapeutic composed of a combination of the fibrillin-1 peptides of interest that would allow patients suffering from congenital heart disease or myocardial infarction to recover from cardiomyocyte loss. In the case of CHD specifically, a treatment like this could be extremely effective in pediatric patients, as their cECM composition is closer to what is seen developmentally than adult cECM is.

Unifying Figure:



Unifying Figure: The percent of cardiac cells that proliferate compared to the age of the rat shows a significant decrease between fetal (80%) and neonatal (70%) and a significant decrease to 0% proliferation from neonatal to adult cells. Fetal and neonatal rats proliferate and regenerate cardiac tissues while adult rats differentiate into scar tissue. Previous research has potentially linked this characteristic to a sequence of proteins in fibrillin 1 which we hypothesize inhibits TGF-B, preventing differentiation.

SPECIFIC AIMS:

Aim #1: Determine the relationship between TGF-B and F1R1 in terms of cardiac cell proliferation and activation. We hypothesize that in the neonatal cell environment, F1R1 binds to TGF-B and promotes proliferation by inhibiting fibrosis. We hypothesize that introducing TGF-B to neonatal cardiac cells will result in a decrease in proliferation and an increase in differentiation compared to the control. Adding both F1R1 and TGF-B will lead to F1R1 inhibiting TGF-B and thus an increase of proliferation and decrease of differentiation compared to TGF-B alone and similar rates compared to the control. The control, F1R1, and both F1R1 and TGF-B groups are expected to have a proliferation rate of $14.8 \pm 3\%$ ¹ of cells and a differentiation rate of $20 \pm 4\%$ ¹⁵ of cells. The TGF-B group is expected to have a proliferation rate of 9.5% of cells and a differentiation rate of 80% of cells. Ki67 stain (proliferation stain) will be used in conjunction with SMA stain (differentiation stain) to understand the trends of proliferation and scar tissue formation. F1R1 has been shown to promote proliferation in previous studies¹. Understanding the mechanisms of action through which F1R1 promotes proliferation will provide insight into the regenerative properties of the neonatal heart and will be essential for the potential application of the peptide in therapeutics. This aim will partially explain the absence of proliferation in mature cardiac cells and provide a basis for developing methods to restore proliferation. If our hypothesis is correct, scar tissue inhibition is one of the mechanisms by which cardiac cells proliferate after injury or malformation.

Aim #2: Identify cardiac cell signaling pathways that are significantly influenced by F1R1. Our working hypothesis is that F1R1 treatment alone should have some effect on the differentiation pathways in cardiac fibroblasts. We would expect to see some sort of downregulation in proteins associated with myofibroblast development after F1R1 treatment of TGF-b-exposed fibroblasts, specifically the SMAD and MAPK protein families¹⁷. In the case of the former, TGF-b binding induces Smad 2, 3, and 4 to form a complex that then goes on to bind to promoter sequences associated with the myofibroblast phenotype, increased matrix deposition, and therefore increased fibrosis in the heart. TGF-B can also initiate SMAD-independent pathways like PI3K/Akt and MAPK cascade components like ERK 1/2 and p38 MAPKs, which drive fibroblast activation on their own or pass on their signal to the SMAD pathway^{2, 14, 4}. Furthermore, differentiation-inducing signals can also be generated by fibroblast mechanosensing, highlighting proteins like RhoA/ROCK and YAP/TAZ as potential targets of F1R1^{4, 5}. As a result of these factors, our primary focus will be on SMADs 2 and 3, but proteins involved in non-canonical TGF-b signaling and mechanoregulation must also be considered. Therefore in a Western blot experiment with two sets of F1R1-treated, scrambled F1R1-treated, and untreated cardiac fibroblast lysate, one of which will be exposed to TGFb, the F1R1-treated groups should exhibit a lower intensity band for at least one of the previously mentioned signaling elements when compared to the control and scramble-treated groups not treated with F1R1. Including a scrambled F1R1 group will reveal if any cellular changes are bought on by protein treatment itself, rather than the native structure and properties of F1R1. This will give insight into how F1R1 treatment promotes an anti-fibrotic phenotype in both the absence and presence of exogenous TGF-B and which downstream signaling elements are hindered. Characterizing the mechanism of F1R1 action in cardiac cell cultures in terms of its downstream effects will help to translate its effects to mature tissue and eventually the clinical setting.

Aim#3: Determine the effect of increasing F1R1 concentration past physiological standards. We hypothesize that the rate of proliferation will increase as the concentration of F1R1 increases. Based on past literature, a concentration of 50 ug/ml of F1R1 within a cardiac fibroblast culture accurately depicts a neonatal rat cECM environment¹³. Although 50 ug/ml is an accurate concentration for biomimicry, we expect that the effects of F1R1 do not falter at higher concentrations. For this experiment, we will use 3

variable groups and a control group. The 3 variable groups will contain varying concentrations of F1R1 (50 ug/ml, 100 ug/ml, and 200 ug/ml). All 3 variable groups and the control group will also contain TGF-B at a consistent concentration of 2.5 ng/ml. The 50 ug/ml F1R1 will represent the current standard and we expect to see similar results as with our previous aims. 100 ug/ml and 200 ug/ml will represent concentrations above the physiological range and will show us if F1R1 continues to increase proliferation as concentration increases. We expect that there will be a significant increase with respect to an increasing concentration between each variable group. From this aim, we hope to better establish a method for future testing of the impact of F1R1 on the rate of proliferation.

METHODS – Experimental Tools, what they are, how they work, how they fit your goals

Cardiac Fibroblast Isolation

The goal of the first experiment is to determine the relationship between TGF-B and F1R1, as outlined in aim #1. The first step of this experiment was to isolate the primary cells for culturing, which were cardiac fibroblasts from rats. The rat pups were euthanized through conscious decapitation before dissecting each neonatal heart using sterile tools. Dissected hearts were then placed in a PBS (phosphate-buffered saline)-glucose solution over ice, allowing the cardiac cells to stay alive while also slowing their metabolic activity. Next, connective tissue was stripped from each heart before removing the top $\frac{1}{3}$ of the tissue to isolate the ventricles alone, which were then placed in a fresh batch of PBS glucose. The ventricle tissue samples could then be minced to increase the surface area available for enzymatic digestion. The minced tissue and all of the PBS solution were then pipetted into a conical test tube. After this, a filtered type II collagenase and PBS glucose solution were added to the sample in 7 mL increments after 7 minutes of incubation to digest the tissue. After the first digestion period, the supernatant was discarded, but in subsequent digestions, the supernatant was collected in a separate test tube and treated with a stop solution to halt enzymatic activity. The digested solution was then pre-plated in DMEM to distinguish and separate cardiac cell populations, with cardiac fibroblasts quickly adhering while cardiomyocytes fail to do so. This solution was then incubated for 4 days before experimentation.

Cell Seeding and Viability Assay

The next step was to harvest the cardiac fibroblasts and seed the cardiac cells in well plates. At this point, the cardiac fibroblasts were all adhered to the bottom of the flask, and the old media was aspirated out. Then, trypsin was added to remove the adherent cells from the bottom of the flask, and new media was added to deactivate the trypsin. The cells were then removed along with the new media, put into a conical, and centrifuged to obtain a cell pellet. A live/dead assay was then performed on the cells within the cell pellet by staining with tryptophan blue and using the Countess machine to determine cell concentration and viability. The concentration of live cells determined the amount of media needed to reach the desired concentration of $0.05e^6$ cells per individual well. The media was added to each well first, and the cells were subsequently added. After viewing the cells under a microscope to verify an appropriate concentration and lack of clumping, 3 full well plates were seeded with the cardiac fibroblasts to create 72 individual samples. These well plates were left in the incubator for 24 hours and then removed from the incubator to swap the serum-containing media in the cell plates with serum-free media. Serum-containing media has many growth factors that help cells grow and proliferate, so it is good practice to replace the media after 24 hours to reduce the number of variables that may cause cell growth among the different experimental groups. The cells were then put back in the incubator for another 24 hours.

Treatment with Experimental Conditions

After 48 hours of incubation, experimental conditions could begin. First, F1R1 (50 μ g/mL) and TGF-B (2.5 ng/mL) were added to 10mL serum-free media vials. These concentrations were determined to be optimal from previous experiments in the Black Lab¹. Then, one of the well plates was taken out of the incubator and viewed under a microscope to verify cell population, morphology, and density. The

media was aspirated, and the cells remained adhered to the bottom of each well. 500 μ L of media with growth factors were added to each well. The cells in the top row of each well plate were the control group and were treated with standard media alone. The cells in the second row of each well plate were treated with F1R1-containing media, the cells in the third row were treated with TGF-B-containing media, and the cells in the bottom row were treated with media containing both F1R1 and TGF-B¹⁸. Each of these experimental groups used only serum-free media. This setup will allow for the comparison of each factor and the observation of any synergistic or inhibitory effect on proliferation or differentiation. The cells were then put back into the incubator for 48 more hours.

Fixing and Staining

To fix the cardiac fibroblasts for staining and imaging, all cells were treated with paraformaldehyde after aspirating the culture media. After this, the cells can be stored at 4°C until the staining procedure can be carried out. 24 hours later, 1 well plate was permeated with triton X-100 and blocked with 5% donkey serum in 1% BSA (bovine serum albumin) in 1x PBS overnight at 4°C on a shaker. The next day, primary rabbit antibodies were added to adhere to Ki67 markers (to detect proliferation), and primary mouse antibodies were added to adhere to aSMA markers (to detect differentiation). After 24 hours at 4°C on a shaker, the primary antibody solution was aspirated and the cells were washed such that only the primary antibodies remained attached to the cells. Then, anti-rabbit and anti-mouse secondary antibodies were added to each well. These secondary antibodies bind to the primary antibodies, and each contains a fluorescent marker at different wavelengths that will be detected during imaging. The cells with the secondary antibody solution were stored and shaken at 4°C for 3 hours before imaging.

Image Analysis

Due to supply chain issues with the aSMA and Ki67 antibodies, imaging with the Keyence was delayed and one culture plate was compromised during the wait. Within each well, one location was selected for imaging in each of four different regions: north, south, east, and west. When choosing a representative sample of cells, only the DAPI overlay was applied to the plate to prevent bias in selection. Also, similar cell densities were maintained for each well region sample image within a condition. At each capture point, four images were generated by the Keyence program that distinguished the stain of interest (DAPI, aSMA, Ki67). This process was repeated for each of the 24 wells (so far) on the plate, yielding 16 images per well. Next, these images were transferred to Cell Profiler software, where the total number of cells could be determined by analyzing the DAPI-stained image. The number of cells positive for aSMA and Ki67 could then be determined through masking and then used to calculate the percentage of fibroblasts that are actively proliferating and/or have differentiated. Instead of the default thresholding method, the Otsu strategy which divides pixels into two or three classes was used. Another parameter change that was useful was decreasing the threshold correction factor, which at default assumes that 50% of the input image is populated with objects. Another issue pointed out by our advisor was in the aSMA staining, where there was a good degree of background staining amongst high-intensity “true” aSMA-positive cells. However, in order for a cell to be recognized, these high-intensity regions must overlap with the cell nucleus, which is not always the case. To correct this issue, the watershed algorithm was used to identify aSMA-staining cell bodies based on the location of the DAPI-stained nucleus.

Repeated Experiment w/ Serum-Containing Media

The only new element in this iteration of the experiment will be that the fibroblasts will be completely cultured in serum rather than including a serum starvation step. With this, we hope to reduce the amount of control differentiation so that the relationship between TGF-b and F1R1 can be more clearly seen in our experimental groups. In the first experimental runs of this semester, we ran into a few procedural errors that can be explained by a lack of experience conducting this protocol independently. Firstly, after permeating the cells in preparation for imaging, we only rinsed the solution with PBS 1 time instead of the 3 rinses that the protocol calls for. Because of this, we did not completely remove all of the

unwanted contaminants in our solution and this interfered with the imaging. Secondly, in one of our well plates, we used Ki67 anti-rat secondary antibodies. Because the host cells being imaged are rat cells, this can lead to over-fluorescence as the antibodies can bind to the cells in nonproliferative nuclei. Lastly, we did not have access to the Keyence microscope the day we expected to image our cells. Although it is expected that the secondary antibody can last multiple days, in the future we will plan ahead to align Keyence access with our experimental timeline. The results from these procedural errors were that the cells had poor distribution on the surface of the well and the images contained some unexpected contaminates and excess fluorescence. When re-running this second experimental iteration, we employed the proper PBS washing protocol and used antibodies not from the host species. Nonetheless, the resulting cell growth was still unevenly distributed across the well, with a high density of cells around the edge of each well.

Cell Lysis for Western Blot

Six flasks of cardiac fibroblasts were first isolated from tissue and incubated as previously described. After confluence was confirmed under a microscope, the experimental conditions were established. Due to the abundance of cells when compared to previous experiments, it was decided to directly treat the fibroblasts with TGFb/F1R1 directly in the flask instead of plating beforehand. TGFb was administered at 2.5 ug/mL into three of the flasks, while F1R1 and scrambled F1R1 were introduced at 50 ug/mL for two of the TGFb-containing flasks and two of the three remaining untreated flasks. After this, the cells were placed back into the incubator for a day to ensure proper integration of the treatment solutions. Then, the flasks were washed with PBS 2 times to ensure that all media had been removed. To remove the fibroblasts from the bottom of the flask, trypsin was added at 9 mL per flask and then deactivated with an equal amount of media. Following this, the cold lysis buffer mixed with protease inhibitors was added at 4 mL per flask and the resulting cell solution was placed into 6 separate concials and refrigerated. To ensure that all cell debris was eliminated from the lysate samples, each conical was spun on a centrifuge at 12,000 rpm for 5 minutes and then the supernatant was collected, transferred, and froze as the final lysate product.

Microplate BCA Assay

First, the six lysate samples corresponding to each condition were left in the incubator at 37 °C to thaw. After this, the nine standards of diluted bovine serum albumin (BSA) were created by dissolving different amounts of it into a fixed volume of PBS. The resulting standards had a final BSA concentration of 0, 25, 125, 250, 500, 750, 1000, 1500, and 2000 ug/mL. Next, the BCA working reagent was formulated by mixing BCA Reagent A with BCA Reagent B at a ratio of 50:1. Moving on, the standards and lysate samples were transferred to a 48-well plate at 50 uL per well, followed by treatment with 400 uL of working reagent. To ensure proper mixing of the two solutions, the plate was then placed on a plate shaker for 1 minute and then incubated for 30 minutes. After letting the plate return to room temperature, its absorbance at 562 nm was measured using the plate reader. To generate a standard curve, the absorbance measurement of the 0 ug/mL BSA standard was subtracted from the other absorbance measurements and then plotted against the known concentrations of each standard (Appendix 2). Using this, we determined the protein concentration of the lysate to be too dilute. Given our estimated protein concentration, we would need to inject 62 uL of lysate per gel loading, while the capacity is closer to 40 uL.

Dose-Dependency of F1R1:

Due to the lack of time left to perform both lysate collection and gel electrophoresis, we quickly pivoted to an experiment exploring the dose dependence of F1R1. In this, our senior lab members had questioned whether the 50 ug/mL concentration of F1R1 was optimal, and if higher concentrations could induce a greater effect. First, neonatal rat cardiac fibroblasts were isolated, cultured, and then reseeded into a 12-well plate at a density of 140,000 cells per well. 48 hours after seeding the experimental conditions were established by treating all wells with TGFb at 2.5 ng/mL and then F1R1 at 0, 50, 100,

and 200 μ g/mL. With this setup, it can be seen if increasing F1R1 concentration also increases the potency of its anti-activating effect on cardiac fibroblasts. After letting the TGFb and F1R1 fully integrate into the culture, they were stained with anti-rabbit aSMA and Hoechst overnight to measure differentiation and live nuclei. However, upon imaging with the Keyence, we discovered that the cells had become overly confluent at some point. Due to this, the culture was multilayered rather than monolayered as intended, causing the imaging software to focus on the “peaks” of cells rather than those at the bottom of the plate (Appendix 5). Analysis in CellProfiler was attempted, but the absence of darkness in most images made it impossible for aSMA to be recognized as a cellular object.

RESULTS:

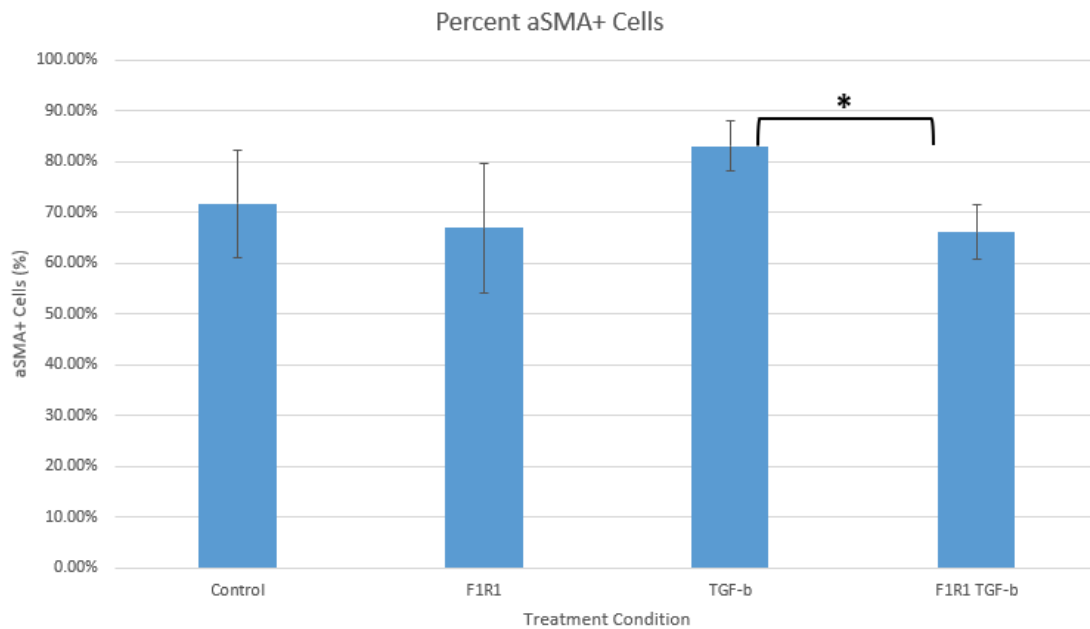


Figure 1: Extent of Cardiac Fibroblast Differentiation for each Experimental Condition. Within each experimental cohort, the percentage of differentiating cells was represented by dividing the amount of aSMA **and** DAPI positive cells by the amount of live cells (DAPI+) on a well-by-well basis. The length of each error bar is two standard deviations about the mean % of aSMA+ cells for each experimental group.

Figure 1 depicts the results of aSMA staining in each of the cultured cardiac fibroblast treatment groups. The percentage of aSMA-positive cells is a reflection of the extent of differentiation of fibroblasts into myofibroblasts. It was expected that the differentiation seen in the TGF-B/F1R1 group should be similar to that of the control due to the anticipated inhibitory action of F1R1. Additionally, the highest amount of aSMA positivity was predicted to occur in the TGF-B-only group, as fibroblast activation by TGF-B has nothing impeding it. In the experimental data, these trends were validated. First, the TGF-B treatment group exhibited a greater average percentage of aSMA positivity than the control by 11.35%, confirming that the cardiac fibroblasts respond to TGF-B activation and differentiate. Furthermore, the F1R1/TGF-B condition had a lower average percentage of proliferating cells when compared to the TGF-B-only group by 16.9%. In this, the experimental evidence suggests that F1R1 can impede TGF-B activation of cardiac fibroblasts. Statistical analysis of the aSMA data supports this as well, with a one-way ANOVA test yielding a p-value of 0.015, indicating that at least one of the experimental groups had a significantly different mean aSMA positivity than the others. Additionally, post hoc analysis revealed that there was a significant difference in the aSMA positivity between the TGFb and F1R1/TGFb at a p-value of 0.0002. However, an unexpected result is the basal level of differentiation seen in the control. With no experimental stimulation, 71.7% of fibroblasts were positive for aSMA on average. A

potential contributor to this could be the stress caused by the serum starvation stage performed during the culturing process.

Source of Variation	SS	df	MS	F	P-value	F crit
Between Groups	0.109808007	3	0.036602669	4.468798196	0.014756259	3.098391212
Within Groups	0.163814374	20	0.008190719			
Total	0.273622381	23				

Table 1: One-way ANOVA of aSMA Data for the TGF-B/F1R1 Experiment. This statistical testing was carried out using the average percentage of aSMA+ fibroblasts for each well within the four experimental conditions. The null hypothesis is defined as all conditions not having significantly different means, with the rejection threshold being a p-value of less than 0.05.

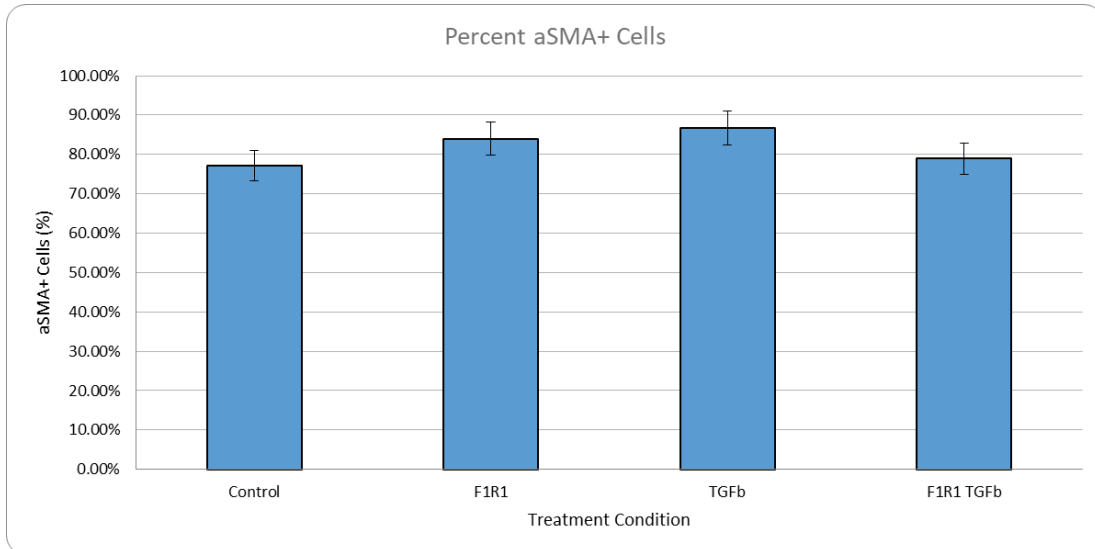


Figure 2: Extent of Cardiac Fibroblast Differentiation for each Experimental Condition. Repeat of Figure 1, but with serum media to potentially reduce basal differentiation.

Figure 2 shows the results of rerunning our initial experiments with serum media instead of serum-free media. The results are similar to last semester's iteration, with a decrease in % of cells differentiating from the TGFb condition (~80%) to the F1R1/TGFb condition (~73%). However, the extent of this inhibitory effect is less than half of what we observed previously in serum-free media (~8% vs ~17%). Additionally, the level of basal differentiation was nearly identical in both versions of the experiment with a differentiation rate of about 72% in the control. An unexpected result is the uncharacteristically high amount of differentiation in the F1R1-only condition, which has an average differentiation rate ~3% lower than that of the TGFb group. It would be expected that F1R1 should induce a level of aSMA positivity similar to the control, so this outcome could have been influenced by other experimental factors that will be mentioned in the discussion. The distribution of cells could have contributed to this, as we observed that cell growth occurred predominantly around the edge of wells with the center remaining sparse (Appendix 3). As a result, the cell count differed enormously between some images and the standard deviation of live cells per well was quite large (~100). To ensure that the data was not biased by sparser images, extreme outliers with cell counts below 40 were excluded from analysis (Appendix 4). A general trend revealed by comparing these results to the serum-free experiment is that the F1R1 and combined treatment groups experienced a greater extent of differentiation in the serum media. However, due to the lack of statistical significance made evident by post hoc testing, concrete relationships between groups cannot be established with confidence. Therefore, the main takeaway from this experiment is that the basal differentiation in the control was not ameliorated by the change in media, justifying another Black Lab member's pursuit of developing silk hydrogels for cardiac cell culturing.

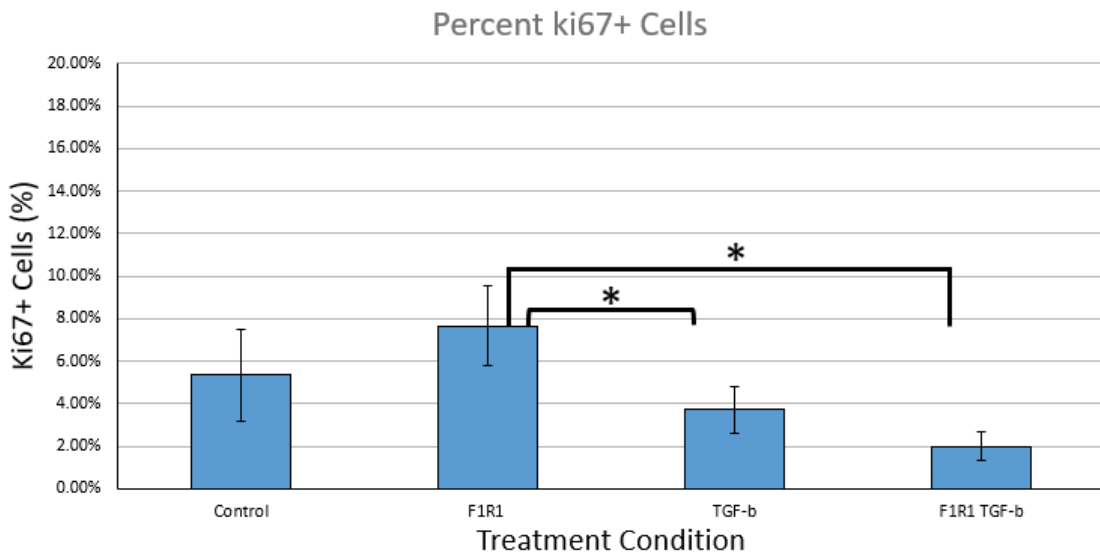


Figure 3: Extent of Cardiac Fibroblast Proliferation for each Experimental Condition. Percentage of proliferating cells was represented by dividing the amount of Ki67 and DAPI-positive cells by the number of live cells (DAPI+).

Figure 3 depicts the proliferative response of cardiac fibroblasts under each experimental condition. We found that treatment with F1R1 alone caused a roughly 1.5-fold increase in the fraction of cells that were proliferating when compared to the control. When comparing the F1R1-only cells to the F1R1/TGFb cells, it can be seen that the addition of TGFb steers the cells away from a proliferative phenotype, causing a ~3.5-fold decrease in the percentage of Ki67+ cells. However, the reverse is not the case, as comparing the TGFb group to TGFb/F1R1 reveals that they differ by less than one percent in terms of the percentage of cells undergoing proliferation. Finally, the amount of proliferation in the control was surprisingly closer to that of the F1R1-only group than the other two groups. So, a major takeaway is that TGFb can nullify the proliferative effects of F1R1 in cardiac fibroblasts, while F1R1 can nullify the activating effects of TGFb. In this way, these two factors work against the phenotype elicited by the other. Post hoc analysis of an ANOVA test elucidated that there was a significant difference between the Ki67 positivity of the F1R1 group compared to the TGFb and F1R1/TGFb conditions at p values less than 1% (Table 2). This supports that F1R1 has an opposing effect to TGFb in terms of both differentiation and proliferation.

DISCUSSION:

The statistically significant changes in the aSMA percentage of cells agree with our hypothesis. The percentage of cells differentiating decreased with the addition of F1R1 or both F1R1 and TGF-B and increased with the addition of TGF-B (Figure 1). TGF-B exposure was expected to increase differentiation as it stimulates a known cardiac fibroblast pathway that results in activation and differentiation into myofibroblasts¹⁴. Testing the influence of F1R1 on fibroblast differentiation contributes to the novelty of this study. There was a significant decrease in differentiation observed in the F1R1 group, suggesting that there is some sort of anti-differentiation mechanism invoked by F1R1.

POST-HOC TEST		
Groups	p-value (T test)	Significant?
Control v F1R1	0.1345664283	No
Control v TGF-b	0.242223775	No
Control v F1R1 TGF-b	0.05021710836	No
F1R1 v TGF-b	0.002249721133	Yes
F1R1 v F1R1 TGF-b	0.0003583249865	Yes
TGF-b v F1R1 TGF-b	0.0128240179	No

Test	Alpha
ANOVA	0.05
Post-hoc (Bonferroni)	0.008333333333

Table 2: Post Hoc Analysis of Ki67 Data.
The Bonferroni corrected alpha threshold to glean significance is $p < 0.0083$.

Furthermore, the decreased differentiation from the F1R1/TGF-B group to a similar level to the control suggests that F1R1 impedes the ability of TGF-B to activate fibroblasts. The downregulation of TGFb-mediated differentiation from the TGFb to F1R1/TGFb condition was also found to be statistically significant at an extremely low p-value ($p = 0.0002$). This mechanism could occur in many different ways, whether it be through direct inhibitory binding of F1R1 to TGF-B or by F1R1 mediating an inhibitory interaction between TGF-B and another cellular factor. Further experiments could focus on determining in what manner F1R1 interacts with TGF-B to curb fibroblast activation. Nonetheless, the decrease in fibroblast differentiation exhibited between the TGF-B and TGF-B/F1R1 groups indicates that F1R1 could effectively reduce scar tissue formation in vivo by acting on TGF-B.

Initial analysis of the control group from aSMA data indicates a high level of basal differentiation at 71.7% (Figure 1). This is substantially higher than some previous studies have shown for cardiac fibroblast differentiation. For example, Li et al. found a basal level of differentiation to be around 20%¹⁶ for neonatal rat cardiac fibroblasts. There are a few possible reasons for this discrepancy. Firstly, Li's study cultured the rat cardiac cells using fetal bovine serum, meanwhile, the cells in this first experiment were cultured in serum-free media. The media used can have a significant effect on the rate of differentiation for a cell culture¹⁷. Thus, the serum starvation stage performed during our culturing process could have affected the basal level of differentiation. Further factors, such as handling and preparation of the cell cultures, can also result in a change in the differentiation rate. The methods used for handling cell cultures were very similar between our experiment and what has been seen in previous studies. However, cell cultures are sensitive to relatively small changes in the environment and/or physical stimuli¹⁸. It is possible that cardiac cells could have been driven to differentiate from accidental stimuli during the preparation process. Another factor that can potentially cause differentiation is intercellular interactions. The proximity of cells to one another can increase or decrease the basal level of differentiation¹⁷. Since this is not a factor that we controlled for, this could have increased the rate of differentiation in our culture.

In order to address the potential effect of serum starvation on cardiac fibroblast differentiation, we reran the same experiment but with serum-containing media. Although the magnitude was lesser, there was still a decrease in aSMA-positive cells from the TGFb to the TGFb/F1R1 treatment groups. Despite this, post hoc testing did not find statistical significance when comparing the extent of activation in these groups. Thus, it is yet to be confirmed if F1R1's dampening of the TGFb-induced cardiac fibroblast differentiation is reproducible in serum-containing media. A more broad takeaway is that there was still a high level of basal differentiation of ~72% in the control even with the media change (Figure 2). These findings suggest that serum starvation did not influence the activation of the fibroblasts in culture and that other factors may be at play. In itself, the introduction of serum comes with some limitations. Serum contains hormones, growth factors, and many other undefined substances that may influence the differentiation or proliferation of cardiac cells¹⁹. There is not expected to be any interference with serum media and the treatments we used. Because of these limitations, serum-free media is the standard in the field once serum starvation is found to not affect the data²⁰. Moving forward, serum-free media would be preferable for these fibroblast experiments to reduce differentiation and proliferation not induced by TGFb or F1R1 treatment. This conclusion is further supported by our attempted F1R1 dose dependency experiment with serum, which saw wells become overly confluent despite seeding density being appropriate (Appendix 5).

As previously mentioned, cells in close proximity can also influence each other's phenotype through intercellular signaling. Furthermore, the distribution of cells in each well was irregular in this experimental iteration, with growth only occurring on the perimeter of each well and the center remaining unpopulated. With this in mind, the denser areas of cells at points around the edge could have bolstered the signaling cues exchanged between fibroblasts, resulting in more ensemble differentiation. Taking the unexpectedly high differentiation in the F1R1-only condition into account, aggressive treatment could

have put excessive stress on the cells, pushing them to differentiate. Another factor at play here could be the reaction of the cardiac fibroblasts to tissue culture plastic (TCP). TCP can have a stiffness of up to 3 GPa while a healthy cardiac environment is closer to 7 kPa, which could be triggering the mechanosensing pathways of fibroblasts to induce the myofibroblast transition²¹. These results and subsequent considerations show that our colleague Benjamin Hoang's pursuit of designing silk hydrogels for optimal cardiac cell growth is justified.

Unlike the first iteration, we were able to extract meaningful data about the effects of F1R1 and TGFb on cardiac fibroblast proliferation with Ki67 staining. Specifically, there was a significant difference in Ki67 positivity between the F1R1 condition and both the TGFb and F1R1/TGFb groups (Table 2). This suggests that F1R1 is able to upregulate proliferation-promoting pathways in cardiac fibroblasts while TGFb has an opposing effect. Although there was no significance between the control and F1R1 conditions, this could have been influenced by the previously mentioned effects of serum media and intercellular signaling. Cardiomyocytes could have a similar response to F1R1 treatment, as they share differentiation and proliferation pathways with cardiac fibroblasts due to their shared progeny²². This cements the potential for F1R1 to be a catalyst for cardiomyocyte proliferation, especially *in vivo* where the massively reduced stiffness would be more favorable towards a proliferative environment rather than a differentiative one.

Our results so far suggest that F1R1 inhibits the TGF-B differentiation pathway. The next steps for this study will be to further investigate and confirm the interaction. While there was no time to perform it this semester, we have already established and obtained an antibody panel of proteins associated with TGFb-mediated activation for a Western Blot experiment.

FUTURE WORK:

While we did not have time to execute it this semester, the Western blot of F1R1-treated, scramble-treated, and untreated cardiac fibroblasts is set up perfectly for future students. Based on the results of the first experiment and previous research in the Black lab, F1R1 has the capability to influence cardiac fibroblast phenotype in the presence and absence of exogenous TGF-b stimulation¹. So, by using antibodies to label proteins involved in fibroblast activation, the downstream targets of F1R1 can be elucidated. The cellular targets we chose and purchased antibodies for were GADPH (loading control), SMAD/pSMAD 2/3, Akt/pAkt, pROCK1, p38 MAPK, YAP, RhoA, ERK 1/2, and TAZ. Upon TGF-b binding, Smad 2 and 3 become activated and complex with Smad 4, which then binds to a promoter sequence associated with fibroblast differentiation and increased matrix output. Fibroblast activation can also be independent of Smad proteins where proteins like MAPK, ERK, and Akt can perform signal transduction from the initial TGF-b binding instead. Other proteins like RhoA/ROCK and YAP/TAZ have implications for both TGF-b and mechanical stress-induced differentiation signaling. For SMAD 2/3, Akt, and ROCK1, the phosphorylated species should be considered to gauge protein activity and the success of TGF-b signal transduction. Since the manner in which F1R1 disrupts TGF-b-mediated activation is unknown, it may act by preventing the activation of key signaling elements.

The next step would then be the RNA-sequencing of F1R1-treated fibroblasts. While the Western blot experiment would be very specific to differentiation pathways, RNA-seq could show what other pathways are influenced by F1R1 to produce a more anti-fibrotic cardiac environment. For this proposed experiment, the same 3 variable groups as aim 2 could be utilized: F1R1-treated, scrambled F1R1-treated, and untreated cardiac fibroblasts. It would be expected that F1R1 would cause a change in the expression of genes normally associated with cardiac differentiation such as Rasl11b, Xylt1, Comp, Nkx2.5, Tbx5, Mef2c, or Tnncl²³. Transcriptome characterization can be carried out by a lab in the Tufts School of Medicine after an adequate amount and quality of RNA has been extracted and purified. This would help to provide a more holistic understanding of the mechanisms of action that F1R1 utilizes to prevent differentiation.

After this, the Black lab will continue to work with F1R1 to gain a better understanding of the mechanisms of action. One hypothesis that will be investigated in the future is that F1R1 prevents the release of TGF-B from the TGF-B latency-associated peptide (LAP). The TGFB LAP holds the TGFB protein and is attached to the Latent TGF-B1 binding protein (LTBP-1)³. We predict that F1R1 binds to either the TGF-B LAP or the LTBP-1. If F1R1 binds to, LTBP-1 it can prevent the complex from binding to the ECM. If the complex cannot gain leverage from the ECM, the TGF-B cannot be released, inhibiting the differentiation of cardiac fibroblasts.

CONCLUSIONS:

- The significant difference between the aSMA positivity in the F1R1 and F1R1/TGFb conditions suggests that F1R1 impedes the ability of TGFb to activate fibroblast and increase their scar tissue production
- In the serum-containing experiment, the persistence of high basal differentiation in the control indicates that it may be attributed to the greater stiffness of TCP compared to the physiological setting.
- The significant increase in proliferation from the TGFb and F1R1/TGFb groups to the F1R1 condition show that F1R1 is associated with increased proliferation in fibroblasts, which is then counteracted by TGFb action.

INDIVIDUAL CONTRIBUTIONS:

Planning - Ryan

Abstract - Joe

Engineering Design Elements - Bailey, Joe

Intro - Joe

Specific Aims - Bailey, Joe

Figures - Bailey, Ryan, Joe

Methods - Ryan, Joe

Image Analysis + Results - Joe

Discussion- Bailey, Joe

Statistical Analysis - Ryan, Joe

Lab Work - Bailey, Ryan, Joe (with help from Nick and Ben)

Poster - Bailey, Ryan, Joe

Website - Ryan

Biweekly Report Work, Other Documentation - Bailey, Ryan, Joe

References:

1. Edmunds, K. J.; Porter, E. C.; Guyette, J.; Jaiganesh, A.; Williams, C.; Ott, H. C.; Weinbaum, J. S.; Black, L. D. The Identification of a Fibrillin-1-Derived Matrix Peptide that Promotes Neonatal Cardiomyocyte Proliferation. (in draft)
2. Yousefi, F., Shabaninejad, Z., Vakili, S., Derakhshan, M., Movahedpour, A., Dabiri, H., Ghasemi, Y., Mahjoubin-Tehran, M., Nikoozadeh, A., Savardashtaki, A., Mirzaei, H., & Hamblin, M. R. (2020). TGF- β and WNT signaling pathways in cardiac fibrosis: Non-coding

RNAs come into focus. *Cell Communication and Signaling*, 18(1), 87.
<https://doi.org/10.1186/s12964-020-00555-4>

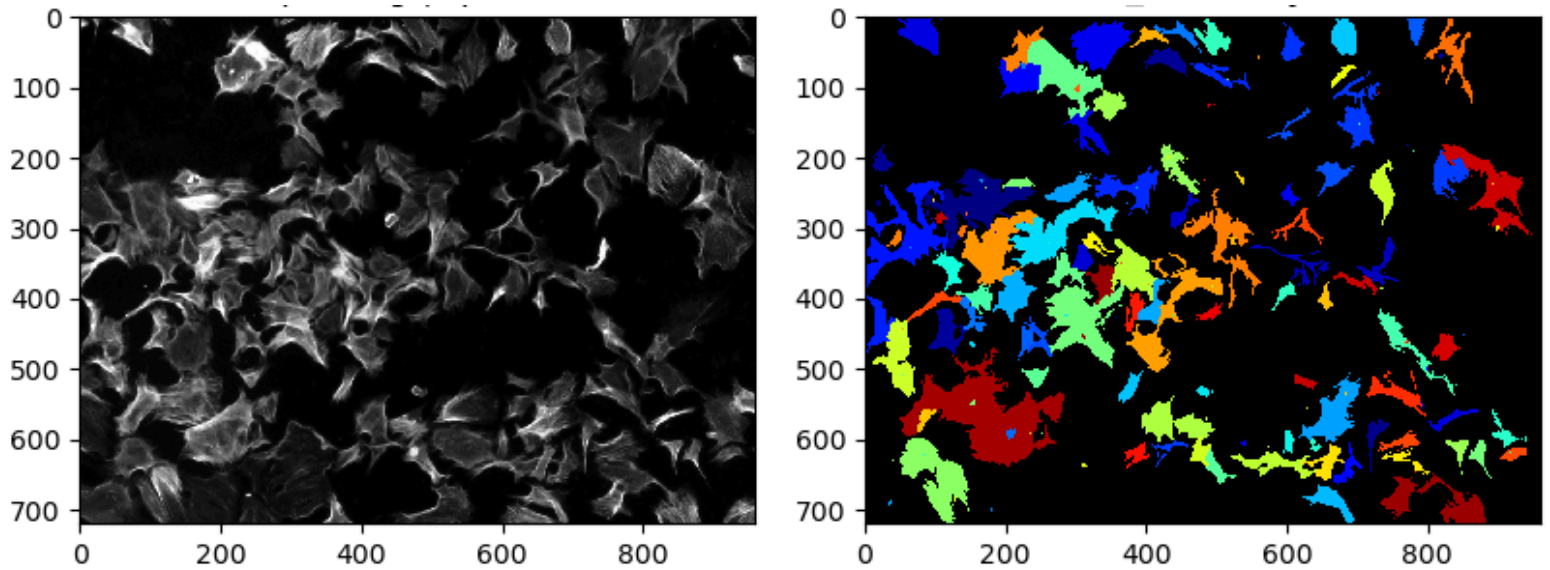
3. Hinz, B. The extracellular matrix and transforming growth factor- β 1: Tale of a strained relationship. *Matrix Biology* 47, 54-65 (2015). <https://doi.org/10.1016/j.matbio.2015.05.006>
4. Umbarkar, P., Ejantkar, S., Tousif, S., & Lal, H. (2021). Mechanisms of Fibroblast Activation and Myocardial Fibrosis: Lessons Learned from FB-Specific Conditional Mouse Models. *Cells*, 10(9), 2412. <https://doi.org/10.3390/cells10092412>
5. Dalla Costa, A. P., Clemente, C. F. M. Z., Carvalho, H. F., Carvalheira, J. B., Nadruz, W., Jr, & Franchini, K. G. (2010). FAK mediates the activation of cardiac fibroblasts induced by mechanical stress through regulation of the mTOR complex. *Cardiovascular Research*, 86(3), 421–431. <https://doi.org/10.1093/cvr/cvp416>
6. Ceccato, T. L., Starbuck, R. B., Hall, J. K., Walker, C. J., Brown, T. E., Killgore, J. P., Anseth, K. S., & Leinwand, L. A. (2020). Defining the Cardiac Fibroblast Secretome in a Fibrotic Microenvironment. *Journal of the American Heart Association: Cardiovascular and Cerebrovascular Disease*, 9(19), e017025. <https://doi.org/10.1161/JAHA.120.017025>
7. Jia T, Wang C, Han Z, Wang X, Ding M, Wang Q. Experimental Rodent Models of Cardiovascular Diseases. *Front Cardiovasc Med*. 2020 Dec 7;7:588075. doi: 10.3389/fcvm.2020.588075.
8. Sengle, Gerhard et al. “Microenvironmental regulation by fibrillin-1.” *PLoS genetics* vol. 8,1 (2012): e1002425. doi:10.1371/journal.pgen.1002425
9. Sun, R.; Liu, M.; Lu, L.; Zheng, Y.; Zhang, P. Congenital Heart Disease: Causes, Diagnosis, Symptoms, and Treatments. *Cell Biochem Biophys* 2015, 72 (3), 857–860. <https://doi.org/10.1007/s12013-015-0551-6>.
10. Isomi, M.; Sadahiro, T.; Ieda, M. Progress and Challenge of Cardiac Regeneration to Treat Heart Failure. *Journal of Cardiology* 2019, 73 (2), 97–101. <https://doi.org/10.1016/j.jcc.2018.10.002>.
11. Xin, M.; Olson, E. N.; Bassel-Duby, R. Mending Broken Hearts: Cardiac Development as a Basis for Adult Heart Regeneration and Repair. *Nat Rev Mol Cell Biol* 2013, 14 (8), 529–541. <https://doi.org/10.1038/nrm3619>.
12. Giacca, M. Cardiac Regeneration After Myocardial Infarction: An Approachable Goal. *Curr Cardiol Rep* 2020, 22 (10), 122. <https://doi.org/10.1007/s11886-020-01361-7>.
13. Williams, C.; Quinn, K. P.; Georgakoudi, I.; Black, L. D. Young Developmental Age Cardiac Extracellular Matrix Promotes the Expansion of Neonatal Cardiomyocytes in Vitro. *Acta Biomater* 2014, 10 (1), 10.1016/j.actbio.2013.08.037. <https://doi.org/10.1016/j.actbio.2013.08.037>.
14. Ma, Z.-G.; Yuan, Y.-P.; Wu, H.-M.; Zhang, X.; Tang, Q.-Z. Cardiac Fibrosis: New Insights into the Pathogenesis. *Int J Biol Sci* 2018, 14 (12), 1645–1657. <https://doi.org/10.7150/ijbs.28103>.
15. Li J, Zhang W, Jiao R, Yang Z, Yuan Y, Wu Q, Hu Z, Xiang S, Tang Q. DIM attenuates TGF- β 1-induced myofibroblast differentiation in neonatal rat cardiac fibroblasts. *Int J Clin Exp Pathol*. 2015 May 1;8(5):5121-8. PMID: 26191207

16. Hagmann, S., Moradi, B., Frank, S. et al. Different culture media affect growth characteristics, surface marker distribution and chondrogenic differentiation of human bone marrow-derived mesenchymal stromal cells. *BMC Musculoskelet Disord* 14, 223 (2013).
<https://doi.org/10.1186/1471-2474-14-223>
17. Maul, Timothy M et al. "Mechanical stimuli differentially control stem cell behavior: morphology, proliferation, and differentiation." *Biomechanics and modeling in mechanobiology* vol. 10,6 (2011): 939-53. doi:10.1007/s10237-010-0285-8
18. Saadat, S., Noureddini, M., Mahjoubin-Tehran, M., Nazemi, S., Shojaie, L., Aschner, M., Maleki, B., Abbasi-kolli, M., Rajabi Moghadam, H., Alani, B., & Mirzaei, H. (2021). Pivotal Role of TGF- β /Smad Signaling in Cardiac Fibrosis: Non-coding RNAs as Effectual Players. *Frontiers in Cardiovascular Medicine*, 7.
<https://www.frontiersin.org/articles/10.3389/fcvm.2020.588347>
19. Barnes, D. & Sato, G. Serum-free cell culture: a unifying approach. *Cell* 22, 649-655 1980.
<https://www.sciencedirect.com/science/article/abs/pii/0092867480905401>
20. Rashid, M-u, Coombs, KM. Serum-reduced media impacts on cell viability and protein expression in human lung epithelial cells. *J Cell Physiol*. 2019; 234: 7718– 7724.
<https://doi.org/10.1002/jcp.27890>
21. Landry, N. M., Rattan, S. G., & Dixon, I. M. C. (2019). An Improved Method of Maintaining Primary Murine Cardiac Fibroblasts in Two-Dimensional Cell Culture. *Scientific Reports*, 9, 12889. <https://doi.org/10.1038/s41598-019-49285-9>
22. Hall, C., Gehmlich, K., Denning, C., & Pavlovic, D. (2021). Complex Relationship Between Cardiac Fibroblasts and Cardiomyocytes in Health and Disease. *Journal of the American Heart Association*, 10(5), e019338. <https://doi.org/10.1161/JAHA.120.019338>
23. Inácio, José Manuel et al. "DAND5 Inactivation Enhances Cardiac Differentiation in Mouse Embryonic Stem Cells." *Frontiers in cell and developmental biology* vol. 9 629430. 13 Apr. 2021, doi:10.3389/fcell.2021.629430
24. Sharifi-Sanjani, M., Berman, M., Goncharov, D., Alhamaydeh, M., Avolio, T. G., Baust, J., Chang, B., Kobir, A., Ross, M., St. Croix, C., Nouraie, S. M., McTiernan, C. F., Moravec, C. S., Goncharova, E., & Al Ghouleh, I. (2021). Yes-Associated Protein (Yap) Is Up-Regulated in Heart Failure and Promotes Cardiac Fibroblast Proliferation. *International Journal of Molecular Sciences*, 22(11), 6164. <https://doi.org/10.3390/ijms22116164>
25. Wei, Y.-H., Liao, S.-L., Wang, S.-H., Wang, C.-C., & Yang, C.-H. (2021). Simvastatin and ROCK Inhibitor Y-27632 Inhibit Myofibroblast Differentiation of Graves' Ophthalmopathy-Derived Orbital Fibroblasts via RhoA-Mediated ERK and p38 Signaling Pathways. *Frontiers in Endocrinology*, 11.
<https://www.frontiersin.org/articles/10.3389/fendo.2020.607968>
26. Schafer, S., Viswanathan, S., Widjaja, A. A., Lim, W.-W., Moreno-Moral, A., DeLaughter, D. M., Ng, B., Patone, G., Chow, K., Khin, E., Tan, J., Chothani, S. P., Ye, L., Rackham, O. J. L., Ko, N. S. J., Sahib, N. E., Pua, C. J., Zhen, N. T. G., Xie, C., ... Cook, S. A. (2017). IL-11 is a crucial determinant of cardiovascular fibrosis. *Nature*, 552(7683), Article 7683.
<https://doi.org/10.1038/nature24676>

Appendix:

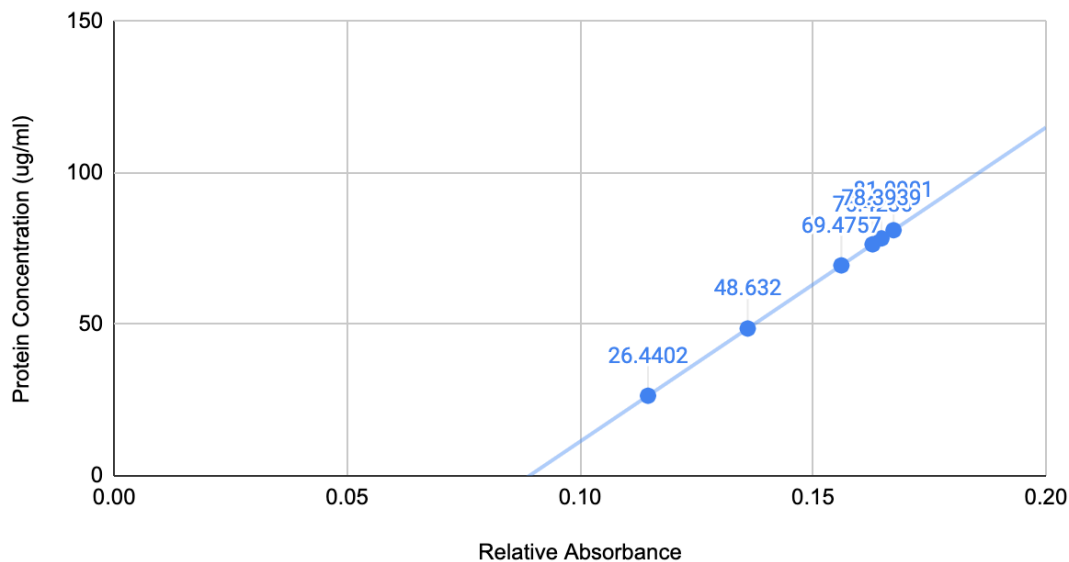
Project Website: <https://sites.tufts.edu/mendingbrokenhearts/>

Project Timeline:

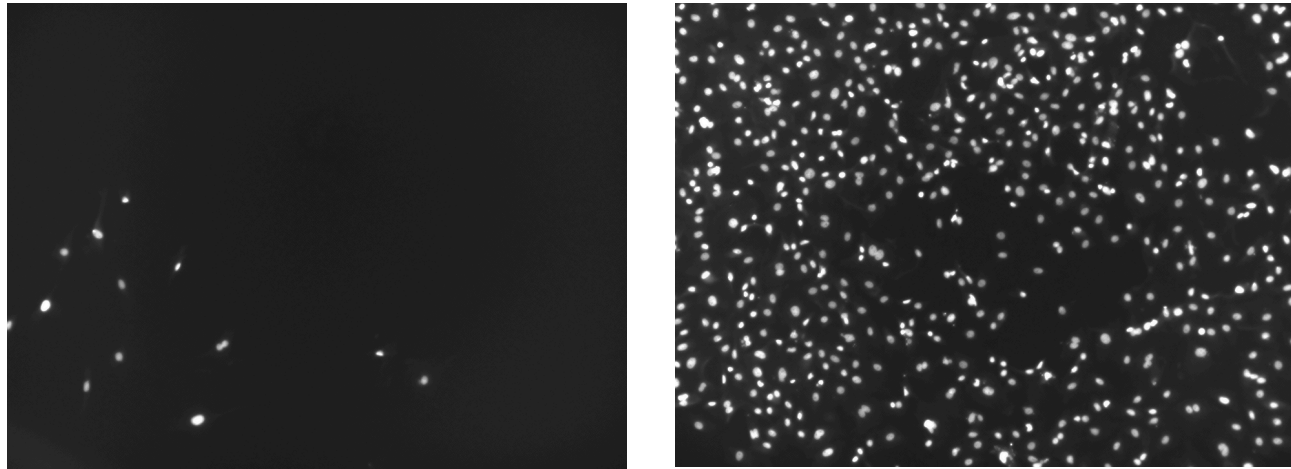


Appendix 1: aSMA Staining and Positive Cell Identification in CellProfiler. The left panel depicts a monochromatic image of aSMA staining. On the right is which cell bodies have been identified as “truly” aSMA positive based on the watershed algorithm, which uses cell nuclei as a seed for secondary object creation.

Protein Concentration (ug/ml) vs. Relative Absorbance



Appendix 2: BCA analysis of the protein concentration in the lysate prepared for a western blot. The protein concentration was compared to a best fit line created by a ladder of known concentrations. The absorbance of the lysate samples were plotted on this best fit line to estimate the protein concentration within each sample.

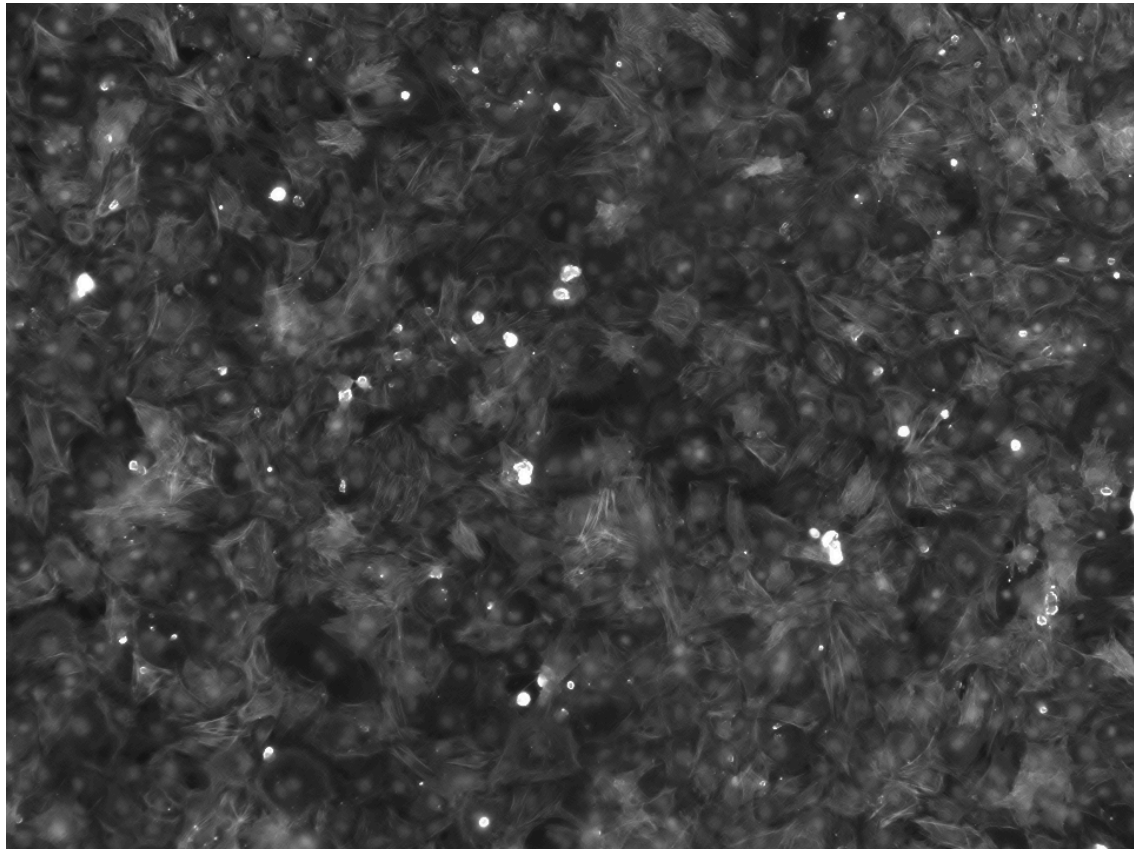


Appendix 3: Example of Extreme Image-to-Image Variation in Cell Count. The DAPI-stained image on the left is from the 5th well of the control group and only has 13 live cells. The right image is from the fourth well of the F1R1/TGFb group and has over 500 live cells as indicated by DAPI staining. This is a consequence of the ring-like growth pattern exhibited in each well.

Condition	Well #	ki67 Positive Cell Count					DAPI Cell Count					% ki67+/Well	Avg Cell Count/Image
		Image #1	Image #2	Image #3	Image #4	Avg	Image #1	Image #2	Image #3	Image #4	Avg		
F1R1 TGF-b	1	1	6		2	3	108	151	54		104	0.0288	104.33
	2		1	3	2	2		87	139	205	144	0.0139	143.67
	3	2	4	4	3	3	141	101	205	149	149	0.0218	149.00
	4	1		14	12	9	99		572	540	404	0.0223	403.67
	5	5	1			3	253	228			241	0.0125	240.50
	6												
TGF-b	1	5	4	3		4	130	102	76		103	0.0390	102.67
	2	2	6			4	166	79			123	0.0327	122.50
	3	7	4	8	0	5	159	164	132	55	128	0.0373	127.50
	4	2	8	15	6	8	68	178	197	131	144	0.0540	143.50
	5	6	1	9	3	5	131	50	230	58	117	0.0405	117.25
	6	4	3	6	0	3	175	136	274	82	167	0.0195	166.75
F1R1	1	12	5	6	8	8	193	148	133	198	168	0.0461	168.00
	2	4	10		17	10	99	88		137	108	0.0957	108.00
	3	9	23	16	13	15	179	187	251	66	171	0.0893	170.75
	4	15	19	14	11	15	172	196	336	57	190	0.0775	190.25
	5	14	18	8	15	14	121	234	50	216	155	0.0886	155.25
	6	13	12	16	13	14	181	177	290	217	216	0.0624	216.25
Control	1	7	2	14	9	8	303	160	480	245	297	0.0269	297.00
	2	6	21	8	2	9	137	301	319	71	207	0.0447	207.00
	3	12	21	9	20	16	187	268	287	196	235	0.0661	234.50
	4	14	12	6	2	9	118	188	71	72	112	0.0757	112.25
	5												
	6												

Sample size selection Experimental selection Visual aberration

Appendix 4: Image Exclusion in Serum-containing TGFb/F1R1 Experiment. Each experimental condition started with six replicates and four images taken within each replicate. The sixth well of the combined condition was excluded from analysis on the basis of procedural errors, as it was only partially treated with F1R1 and TGFb (red row). The images marked by a black box were left on due to their exceptionally low cell count. The average number of live cells per image was ~150 with a standard deviation of ~100 cells, so all images below 40 were omitted. The orange-marked images could not be analyzed because of blurriness or an aberration preventing CellProfiler from making meaningful conclusions.



Appendix 5: Overlay Image from Attempted F1R1 Dose Dependency Fibroblast Experiment. The multitude of out of focus nuclei indicates that there are multiple layers of cells. These fibroblasts were seeded at ~140k cells per well in a 12 well plate, which is above the 100k per well recommended by Thermo Fisher Scientific. This small error was likely exacerbated by the presence of serum in the media, which promotes culture growth.